Elucidating venlafaxine metabolism in the Mediterranean mussel (Mytilus galloprovincialis) through combined targeted and non-targeted approaches

N. Ariza-Castro, Frédérique Courant, Thibaut Dumas, Bénédicte Marion, H. Fenet, Elena Gomez

Title

Elucidating Venlafaxine Metabolism in the Mediterranean Mussel (*Mytilus galloprovincialis*) through Combined Targeted and Non-Targeted Approaches

N. Ariza-Castro [1,3]*, F. Courant[1], T. Dumas[1], B. Marion[2], H. Fenet[1] and E. Gomez[1]

[1]HydroSciences, IRD, CNRS, Université de Montpellier, Montpellier - *nariza@itcr.ac.cr

[2]Institut des Biomolecules Max Mousseron, ENSCM, CNRS, Université de Montpellier, Montpellier, France

[3]Escuela de Química, Instituto Tecnológico de Costa Rica, Cartago 159-7050, Costa Rica

Abstract

Exposure of aquatic organisms to antidepressants is currently well documented, while little information is available on how wild organisms cope with exposure to these pharmaceutical products. Studies on antidepressant metabolism in exposed organisms could generate information on their detoxification pathways and pharmacokinetics. The goal of this study was to enhance knowledge on the metabolism of venlafaxine (VEN)—an antidepressant frequently found in aquatic ecosystems—in *Mytillus galloprovincialis,* a bivalve that is present worldwide. An original tissue extraction technique based on the cationic properties of VEN was developed for further analysis of VEN and its metabolites using targeted and non-targeted approaches. This extraction method was assessed in terms of recovery and matrix effects for VEN metabolites. Commercial analytical standards were applied to characterize metabolites found in mussels exposed to 10 µg/L VEN for 3 and 7 days. Targeted and non-targeted approaches using liquid chromatography (LC) combined with high-resolution mass spectrometry (HRMS) were implemented to screen for expected metabolites based on the literature on aquatic species, and for metabolites not previously documented. Four venlafaxine metabolites were identified, namely N-desmethylvenlafaxine and O-desmethylvenlafaxine, which were clearly identified using analytical standards, and two other metabolites revealed by non-target analysis. According to the signal intensity, hydroxy-venlafaxine (OH-VEN) was the predominant metabolite detected in mussels exposed for 3 and 7 days.

Keywords

Bioaccumulation, pharmaceuticals, metabolites, mass spectrometry, bivalves

Highlights

- An extraction method based on the cationic properties of VEN was successfully developed.
- The non-targeted approach allowed the identification of new VEN metabolites in mussels.
- OH-VEN was the predominant metabolite detected in VEN-exposed mussels.

1 Introduction

Venlafaxine (VEN), an antidepressant prescribed for the treatment of human clinical and anxiety disorders, is one of the most commonly detected pharmaceutically active compounds (PhACs) in the aquatic environment (Brieudes et al., 2017; Moreno-González et al., 2016; Paíga et al., 2019). This contamination affects the coastal marine environment, where recent studies have revealed the bioaccumulation of VEN, among other PhACs, in different species (Alvarez-Muñoz et al., 2015a,b; McEneff et al., 2013). Particularly, bivalves have shown the highest VEN accumulation (up to 36.0 ng/g dw) in relation to other aquatic organisms such as microalgae and fish (Alvarez-Muñoz et al., 2015b). The Mediterranean mussel (*Mytilus galloprovincialis*) is a species commonly used in monitoring environmental contaminants in the marine environment thanks to its wide geographical distribution, its filter-feeding behavior and ability to bioaccumulate contaminants (Gomez et al., 2012; Silva et al., 2016)—it has also recently been used for assessing VEN metabolism. In laboratory VEN-exposed Mediterranean mussels, Serra-Compte et al. (2018) detected three phase I metabolites, i.e. O-desmethyl venlafaxine (ODV), N-desmethyl venlafaxine (NDV) and N,O-didesmethyl venlafaxine (NODDV), while Gomez et al. (submitted) detected four phase I metabolites, i.e. ODV, NDV, NODDV and N,N-didesmethyl venlafaxine (NNDDV). The two previous studies were conducted on the basis of a targeted analysis geared towards monitoring known phase I metabolites, already reported in the literature focused in humans. However, non-targeted approaches are promising to achieve a more complete characterization of VEN metabolism, including previously unreported metabolites in Mediterranean mussels. Non-targeted approaches are based on the generation of chemical profiles in

exposed and non-exposed organisms. Their comparison allow the detection of appearing signals in exposed organisms, those signals corresponding to potential previously unreported metabolites. This strategy helps elucidate biotransformation pathways in mussels, as already demonstrated for diclofenac (Bonnefille et al., 2017). Meanwhile, Jeon et al. (2013) conducted the first experiment to screen for VEN metabolites in freshwater crustaceans with a non-targeted approach using LC-HMRS, and the findings suggested the involvement of biotransformation pathways. These authors documented the structures of five VEN metabolites: three dealkylation products (ODV, NDV and NODDV, confirmed with reference standards) and two hydroxylation products (both with tentatively identified structures). In this context, to our knowledge no studies have focused on the VEN metabolism in mussels using an untargeted approach, thereby highlighting the question as to whether known biotransformation processes in humans are maintained in invertebrates. The goal of the present study was therefore to investigate this strategy for identifying VEN metabolites (already known and non-documented ones) produced in Mediterranean mussels (*M. galloprovincialis*) after exposure. A tissue treatment method based on the cationic properties of VEN and its metabolites (known in humans) was developed to increase the probability of metabolite detection and it was assessed in terms of recovery and matrix effect.

2 Materials and Methods

2.1 Chemicals and materials

VEN (≥ 98.5%), venlafaxine-d6 (VEN-d6, > 98%) and O-demethylvenlafaxine-d6 (ODV-d6, > 99.9%) were purchased from Sigma-Aldrich (Steinheim, Germany). N,N-didesmethyl- O-desmethyl venlafaxine (NNDDODV, ≥98%), ODV-glucuronide (ODV-glucu, > 98%) and NODDV-glucuronide (NODDV-gluco, ≥ 95%) were purchased from Santa Cruz Biotechnology (Santa Cruz, CA, USA), while ODV, NDV, NNDDV and NODDV were obtained at analytical grade (purity ≥ 98%) from Toronto Research Chemicals Inc. (Toronto, ON, Canada). Stock standard solutions of individual compounds were prepared at 100 mg/L concentration in methanol. Subsequent stock standard dilutions were prepared with methanol. All standard solutions were stored at -20°C.

Ultrapure water was generated by the Millipore Simplicity UV system (Bedford, MA, USA) with a specific resistance of 18.2 MΩ.cm at 25°C. Dichloromethane (DCM) as pesticide analytical grade solvent, ammonia (NH_3, 28%) as ACS reagent grade solution and HPLC/MS-grade solvents (methanol-MeOH and acetonitrile - ACN) were purchased from Carlo Erba (Val de Reuil, France).

Formic acid (98% purity) was obtained from Fisher Labosi (Elancourt, France) and ammonium acetate (≥ 98%) was purchased from Sigma-Aldrich (Steinheim, Germany). Dispersive SPE tubes containing Z-Sep-Plus (500 mg/12 mL) was obtained from Supelco (Bellefonte, PA, USA). Oasis® MCX 6 cc (150 mg, 30 µm, 6 cc) cartridges, obtained from Waters Corporation (Mildford, USA), and a Visiprep™ DL Solid Phase Extraction (SPE) Vacuum Manifold from Supelco (Bellefonte, USA) were used for solid phase extraction. All chromatographic solvents were filtered through a 0.22 µm nylon membrane filter (Nylaflo™, Michigan, USA). Glass-fiber filters (0.7 µm pore size) purchased from Whatman (Maidstone, UK) were used to filter seawater.

2.2 Experimental design and sample preparation

M. galloprovincialis mussels were purchased in February 2017 from Mediterranean mussel suppliers (Bouzigues, France) and immediately transported to the laboratory. After cleaning, the mussels were acclimatized in aerated (9.9 ± 0.4 mg/L) filtered natural seawater (salinity = 35 ± 3 g/L, pH = 8.2 ± 0.1 units) for 7 days before the experiment. During the acclimation and exposure periods, the seawater was renewed every day (static renewal), the room temperature was regulated at 15 ± 2°C, and the mussels were fed *Tetraselmis suecica* phytoplankton (Greensea, Mèze, France) at constant density (10,000 cells/mL). 100 mussels (shell length 6.0–7.2 cm) were randomly distributed in 20 glass aquaria at a density of 5 mussels per 2 L water. Two groups were constituted: a solvent control group (with the vehicle for VEN: MeOH) and a group exposed at a nominal VEN concentration of 10 µg/L. Each group consisted of 10 aquaria of 5 mussels each. During the exposure period, the VEN concentration was reestablished after daily water renewal. Seawater samples were taken daily to quantify VEN and its known metabolites. Mussels were sampled at days 3 and 7 of exposure (five aquaria per condition). All mussels were dissected and the digestive gland was frozen at –80°C for further analysis, and the remaining soft tissues (the tissue of interest in our study) were frozen at –80°C before freeze-drying (Heto Power dry LL 3000, Thermo). After lyophilisation, these tissues were homogenized and ground into powder using an MM-2 vibrational mill (Retsch, Haan, Germany). Each sample was then placed inside a clean glass bottle and stored at room temperature in the dark until extraction and analysis. The mussel soft tissue analysis involved five replicates per group (solvent control and exposed) for each day of exposure (3 and 7 days).

2.3 Sample extraction and LC-MS analysis

2.3.1 Tissue extraction method

In order to increase the probability of detection of phase I and phase II (known and unknown) VEN metabolites in mussels, a tissue treatment method was developed using the physicochemical properties of these compounds, especially the positive charge on the amine functional group. 500 mg (± 1 mg) dry weight (dw) of tissue samples obtained by pooling two individuals was weighed in a 50 mL polypropylene centrifuge tube and spiked with VEN-d6 (500 µg/kg) and ODV-d6 (20 µg/kg). The tissues were then extracted by sonication in 5 mL of extraction solvent (5% formic acid in MeOH) for 5 min. The samples were centrifuged at 23°C (3400 x g, 5 min) and the supernatant was decanted in another 50 mL polypropylene centrifuge tube. Re-extraction was carried out for each sample and the resulting supernatants were combined, and then 0.5 g of lipid removal sorbent Z-Sep Plus and 5 mL of 5 mM ammonium acetate were added to the combined supernatant. The sample was then vortexed for 5 min and centrifuged at 23°C (3400 x g, 5 min). The extract obtained was transferred to a glass bottle (250 mL capacity) and diluted with milliQ water to a 150 mL final volume. After dilution, the sample pH was adjusted to 1.4 ± 0.1. Then water-diluted samples were loaded onto the SPE Oasis MCX cartridges pre-conditioned with MeOH (6 mL), milliQ water (6 mL) and 2% formic acid in water (6 mL, pH: 1.40), respectively. After all samples were loaded at a flow rate of 1 mL/min, the cartridges were dried (until there were no longer any drops coming out of them) and then washed with 2% formic acid in water (6 mL, pH: 1.40), MeOH (2 mL), DCM (6 mL) and MeOH (3 mL). The analytes were eluted with 6 mL of 5% ammonium hydroxide in MeOH (5:95, v/v), and the solvent was evaporated to dryness under a gentle N_2 stream at 35°C. The residues were reconstituted with 200 µL of ACN:water (10:90, v/v). Finally, the sample was centrifuged at 13.4 x 10^3 rpm for 10 min to separate the residual lipids. The clear solution was transferred to a vial for LC-MS analysis.

2.3.2 Seawater extraction method

A tailored version of the tissue extraction and cleaning method was applied to determine the real VEN concentration in the seawater sampled during the mussel exposure period. 18 mL of seawater was spiked with surrogate standard (VEN-d6 at 1 µg/L) and ajusted to pH 1.4 ± 0.1. Solid-phase extraction was conducted with the same method used for the tissues, except for the washing step which was performed without DCM (6 mL). The analyte was eluted with fresh prepared ammonium hydroxide in MeOH and the solvent was evaporated to dryness under an N_2 stream. The residue was reconstituted in 200 µL of ACN:water (10:90, v/v) and transferred to a vial for LC-MS analysis.

2.3.3 Liquid chromatography and mass spectrometry conditions

149 Extracts were analyzed on an HPLC Accela 600 pump coupled to a Q-Orbitrap HRMS mass
150 spectrometer (Thermo Fischer Scientific) equipped with a heated electrospray ionization probe (HESI)
151 source for detection. Chromatographic separation involved a reverse phase PFPP analytical column
152 (Discovery HS F5 100 mm x 2.1 mm; 3 µm particle size). The chromatography assays involved a 10
153 µL injection volume, a 0.35 mL/min flow rate and a binary gradient of ACN (A) and water (B), both
154 containing 0.1% formic acid, as follows: 10% A at 0 min, 50% A at 4-6 min, 60% A at 8-10 min, 70% A
155 at 14-16 min, 80% A at 17-19 min, 10% A at 21 min and a stop time at 27 min. Over a 27 min run,
156 data acquisition was performed simultaneously in positive and negative ionisation mode and the HESI
157 parameters were as follows: 55 arbitrary units (AU) sheath gas; 10 AU auxiliary gas; 275°C capillary
158 temperature; 200°C heater temperature, and the electrospray voltage was set at 4.0/–4 kV. The S-lens
159 radio frequency (RF) level was set at 100 AU. Full scan data in polarity switching mode were acquired
160 at a resolution of 35,000 full width at half maximum (FWHM) with an automatic gain control (AGC) of
161 10^6 and 250 ms of the maximum ion injection time. Moreover, MS^2 was achieved using a mass
162 inclusion list composed of the mass of the precursor ion of the compounds of interest. A 10 eV
163 absolute collision energy and 17,500 FWHM resolution of were used. The m/z scan range was set
164 between 50-750.

165 **2.4 Non-targeted metabolite analysis strategy**

166 Chemical profiles from five SC samples and five exposed samples at a nominal VEN concentration of
167 10 µg/L were generated by LC-HRMS for each exposure day (3 and 7 days). The data processing and
168 signal identification strategies were from Bonnefille et al. (2017). Briefly, the data obtained in positive
169 and negative ionization mode were converted with the free MS Convert software package (from *.raw
170 to *mzxml) and extracted using an XCMS script (open source) on the basis of the R software. The
171 XCMS parameters were tailored to fit our data: m/z interval for peak picking of 0.01, signal-to-noise
172 ratio threshold of 5, group band-width of 20, with a 0.4 minimum fraction. After data processing, a 2-
173 dimensional table containing information on each peak was generated (Courant et al., 2014). The
174 peaks detected only in the exposed samples (absent in the control samples) and found in all five
175 replicates were considered as potential VEN metabolites. The resulting signals were confirmed on the
176 basis of the fold change and extracted ion chromatogram. The fold change was calculated as the ratio
177 of the mean signal intensity in exposed samples to the mean signal intensity in the control samples.
178 Only signals with a fold change higher than 10 in negative or positive ionization mode were kept and
179 further processed to determine the structures associated with the signals. Moreover, extracted ion

chromatograms (EIC) were checked manually for all potential signals associated with metabolites so as to confirm the absence of any signal in the controls. Peaks associated with the same molecule (e.g. isotopes and/or dimers) were identified by checking the retention times and shapes of peaks obtained in the chromatograms generated by the Xcalibur QualAnalytical Browser (Xcalibur 3.0, Thermo Fisher Scientific Inc.). The same software was used to determine the elemental composition of unknown metabolites and those with the best fits, along with C, H, N and O compositions that could be related to VEN, are reported in the present study. Chromatographic retention time prediction of unknown metabolites was conducted using the multiple linear regression model developed by Jeon et al. (2013). With this model, an equation was obtained by plotting the retention time versus the molecular weight (MW) and the distribution coefficient (log D_{ow}) of the parent compound and its known metabolites. The MW and log Dow values were generated by ACD/ChemSketch (version 12.01).

2.5 Targeted metabolite analysis

2.5.1 LC-MS analysis

In the targeted analysis, only data acquired in positive electrospray ionization mode were considered, as this was the most sensitive mode for the molecules included in this section of the study (VEN and its known metabolites). Each compound was confirmed on the basis of: (1) the retention time, and (2) the mass accuracy (max 5 ppm deviation) of protonated molecules $[M+H]^+$ in full scan MS mode compared to values obtained for the analytical standards under the same analytical conditions.

2.5.2 Quantification of VEN and its known human metabolites in tissues

In order to quantify VEN and its known metabolites in mussel soft tissues, calibration curves were plotted for blank mussel tissues by adding a fixed amount of the internal standards: VEN-d6 (500 µg/kg dw) and ODV-d6 (20 µg/kg dw) and increasing quantities of the target analytes from 0 to 3000 µg/kg dw for VEN, and from 0 to 80 µg/kg dw for its known phase I (ODV, NDV, NNDDV, NODDV and NNDDODV) and phase II (ODV-glucu and NODDV-glucu) metabolites before extraction.

2.5.3 VEN quantification in seawater

In addition, a seawater calibration curve was plotted by adding a fixed amount of internal standard VEN-d6 (at 1µg/L) and increasing quantities (0–15 µg/L) of the targeted VEN analyte in blank seawater.

2.5.3 Method performances

The method performances of both matrices were evaluated by taking into account aspects such as the linearity, limit of detection (LOD) of the methods, absolute recovery, matrix effects and repeatability

	Tissues

per analyte. Linearity was estimated with blank tests and calibration curves in tissues (five levels) at the 250–3000 µg/kg dw concentration range for VEN and 5–80 µg/kg dw for its known metabolites, and in seawater (seven levels) at 0.1–15 µg/L concentration range for VEN. LODs of the tissues and water methods were determined as the concentration resulting in a signal-to-noise ratio of 3 for each analyte. Absolute recoveries were studied by comparison of the signal area of each analyte in blank samples spiked before and after the extraction/purification process, both injected under the same analytical conditions. Matrix effects were evaluated by comparison of the signal area of each analyte in blank samples spiked after extraction/purification with the signal area of each analyte measured in a pure standard injected under the same analytical conditions. Absolute recovery, matrix effects and repeatability of the methods were evaluated by spiking tissues with 20 µg/kg (dw) and seawater with 1µg/L of all compounds in triplicate.

2.6 VEN bioconcentration factor and the mann Whitney non-parametric statistical test

An apparent bionconcentration factor (BCFa) was calculated for VEN as the ratio of the measured concentration in the tissues to the measured concentration in seawater. The mann Whitney non-parametric statistical test was performed to compare the data obtained at 3 days and 7 days. OriginPro 2018 statistical software was used for this test.

3. Results

3.1 Analytical performance

The method performances are shown in Table 1. Both tissue and water methods demonstrated good linearity (r^2>0.98) in the concentration range defined in both matrices for the 8 compounds included in the study. Absolute recoveries of phase I metabolites were higher than 91% in the tissues. Phase II metabolites had a lower absolute recovery (approximately 50%) in this matrix. A medium matrix effect was observed in tissues for all evaluated analytes (suppression between 32% and 59%). The average variability for all analytes evaluated never exceeded 21% in both matrices. The sensitivity of the methods in terms of LOD ranged from <1.0 to 8.0 µg/kg dw in tissues and was 1 ng/L in seawater.

Table 1
Physicochemical properties, retention time, linearity, absolute recovery, matrix effets, average repetability and method LODs and LOQs observed for each molecule in LC-MS Q-Orbitrap.

Analy										LOQ$_{Meth}$ (ng dw)
NODD. glucu[f]	425.47274	426.2122	2,78; 10,24	-3.58	3.96	0.9923	50 ± 7	-48 ± 3	17	8.0
ODV-glucu[f]	439.49932	440.2279	2,78; 9,26	-3.65	4.21	0.9993	49 ± 19	-51 ± 8	16	8.0
NNDDODV[e]	235.32204	236.1645	9,72; 10,38	-1.79	6.96	0.9832	96 ± 4	-59 ± 6	21	3.0
NODDV[e]	249.34862	250.1801	9,83; 10,59	-1.29	7.91	0.9988	98 ± 6	-41 ± 9	4	2.0
ODV[e]	263.3752	264.1958	9,23; 10,04	-1.36	8.02	0.9886	100 ± 5	-32 ± 8	5	5.0
NNDDV[e]	249.34862	250.1801	9,85; 14,75	-1.06	11.64	0.9987	97 ± 6	-55 ± 8	17	0.5
NDV[e]	263.3752	264.1958	10,44; 14,83	-0.55	12.08	0.9945	108 ± 12	-32 ± 12	9	1.5
VEN	277.40178	278.2114	9,26; 14,84	-0.62	14.23	0.9998	105 ± 7	-32 ± 11	4	0.5
					Seawater					
VEN	-	-	-		14.18	0.9992	105 ± 11	14 ± 3	18	1,0 (µg/L)

[a,b,c,d] values predicted with ACD/ChemSketch software; [e]phase I metabolite and [f]phase II metabolite.

3.2 VEN quantification

The VEN concentrations were measured in water to control mussel exposure in aquaria. The exposure concentrations measured in the exposed aquaria ranged from 9.5 to 12.5 µg/L (Table 2). No signal of the parent compound (VEN) was detected in the control samples (SC) of both matrices (seawater and tissues). Mean VEN concentrations in exposed mussel tissues were around 1.9 mg/kg dw and 2.5 mg/kg dw at days 3 and 7, respectively. Moreover, when considering the VEN concentration measured in water and exposed mussel tissues, the apparent bioconcentration factors (BCFa) were 177 ± 27 L/kg dw and 229 ± 29 L/kg dw for days 3 and 7, respectively. Finally, with the Mann Whitney non-parametric statistical test, for VEN and its metabolites ODV and NDV, no significant differences in the concentrations were observed between day 3 and day 7.

Table 2 Mean concentrations of VEN and its metabolites NDV and ODV measured in the different conditions and matrices (seawater and tissue) of the study.

		Analytes		
Matrix	Conditions	VEN (µg/L in water ou µg/kg dw in tissue) (n=5)	NDV (µg/L in water ou µg/kg dw in tissue) (n=5)	ODV (µg/L in water ou µg/kg dw in tissue) (n=5)
Seawater	SC	< LOD	< LOD	< LOD
	Exposure	11.0 ± 1.5	< LOD	< LOD
Tissues	SC	< LOD	< LOD	< LOD
	3rd day of exposure	1948 ± 493	50 ± 13	28 ± 7
	7th day of exposure	2517 ± 341	34 ± 13	24 ± 8

3.3 Non-targeted analysis of VEN and its metabolites in tissues

The non-targeted approach led to the detection of four metabolites. All of these molecules were detected in positive mode, while no signal in the negative mode could be identified as a potential metabolite. The metabolite and parent compound identification process is described below. Relevant information on the identification of these molecules is also presented in Table 3.

3.3.1 Venlafaxine

Among the signals detected in exposed mussels, absent in the control samples and found in all replicates, a peak with molecular mass $[M+H]^+$ 278.2114 was identified at 14.23 min (i.e. M in Table 3). The selection of this signal was confirmed by its fold change value of 132 (value >10) and its extracted ion chromatogram (Fig. 1). Xcalibur software helped determine the elemental composition of the signal and the suggestion with the smallest delta atomic mass unit (amu) was considered. The experimental mass $[M+H]^+$ 278.2114 associated with the retention time (14.23 min) and elemental composition proposed ($C_{17}H_{27}NO_2$) coincided with the identification of VEN (Table 1). The experimental mass of VEN was compared with its theoretical mass and no difference was found (Table 3). The identification of the signal corresponding to the isotopic ion ^{13}C ($[M+H]^+$ 279.2148) at 14.26 min reconfirmed the presence of this molecule (VEN) (Fig. 2). HCD fragmentation (at 10 eV) demonstrated the presence of a fragment at m/z 260.2007 (Fig. 2, (1). This fragment was associated with the loss of 18.0107 amu compared to the measured VEN m/z 278.2114, corresponding to a neutral loss of H_2O in the VEN structure. In addition, the signal corresponding to the isotopic ion ^{13}C ($[M+H]^+$ 261.2039) of this fragment was identified. A second fragment was observed at m/z 215.1427 (Fig. 2, (2)). This fragment corresponded to a loss of 45.0580 amu (equivalent to a loss of C_2H_7N)

283 relative to the previously observed fragment in the VEN structure. A third fragment was found at m/z
284 121.0646 (Fig. 2, (3)). The elemental composition of this fragment corresponded to C_8H_9O. Note that
285 the signals corresponding to the fragments and 13C isotopic ions had peak shapes and retention
286 times very similar to those of VEN, thereby indicating that they were related. The VEN identification
287 was confirmed by injection of the analytical standard under the same conditions reaching the
288 maximum confidence level (level 1) in the identification of elucidated signals from a non-directed
289 analysis, according to the scale proposed by Schymanski et al. (2014).

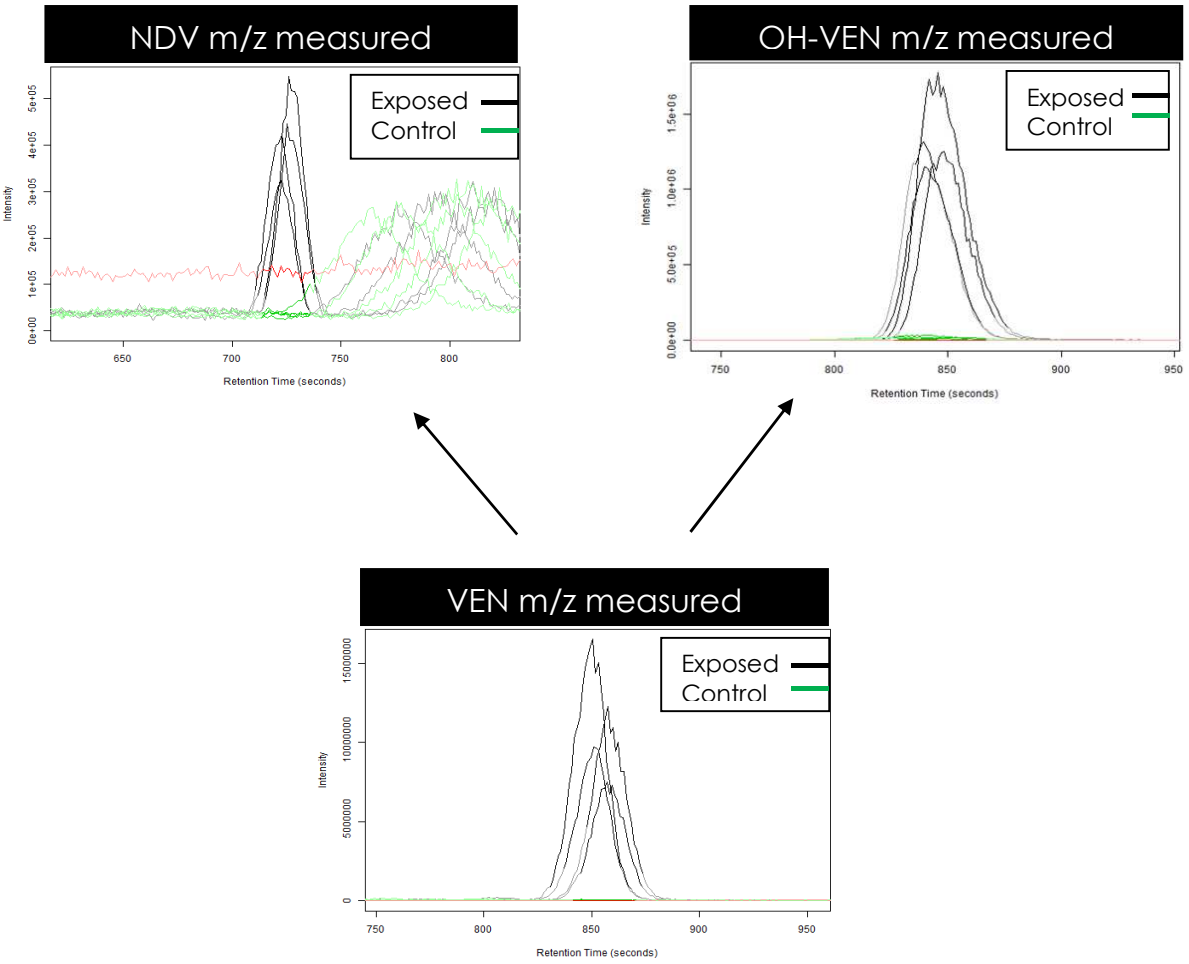

Figure 1.Examples of extracted ion chromatograms of metabolites (NDV and OH-VEN) and the parent compound (VEN). Black peaks represent the exposed samples and green peaks are the control samples. No peaks were identified in the control samples for these molecules.

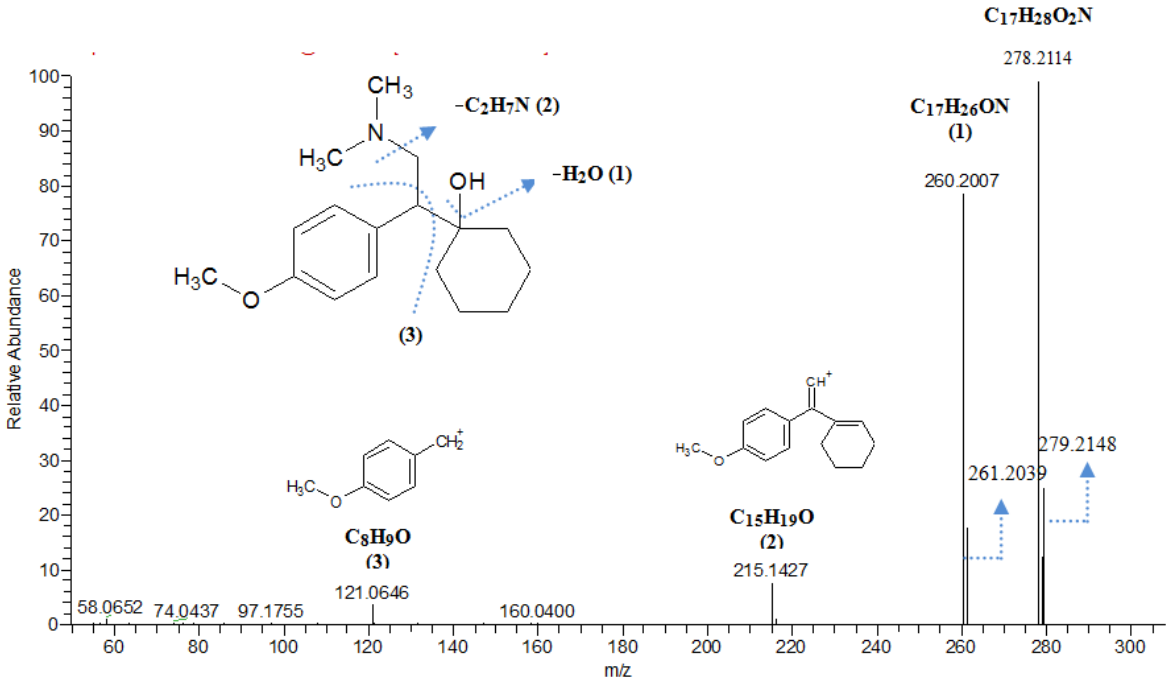

Figure 2. Relevant ions from the high resolution mass spectrum of fragmented VEN at 10 eV

3.3.2 Phase I metabolites

3.3.2.1 Oxidative metabolism-demethylation

Two metabolites identified as M1 and M2 (Table 3) displayed a $[M+H]^+$ of 264.1958. The signals of both metabolites demonstrated a fold change higher than 10 and were detected only in the exposed samples (Fig. 1). They presented a mass decrease of 14.0156 amu (equivalent to a loss of CH_2) compared to the VEN structure, corresponding to dealkylation in the parent compound structure. M1 and M2 exhibited different retention times, indicating that demethylation occurred at different positions. N-demethylation enabled greater interaction of nitrogen-free electron pairs with pentafluorophenyl propyl groups of the stationary phase in the chromatographic column used.

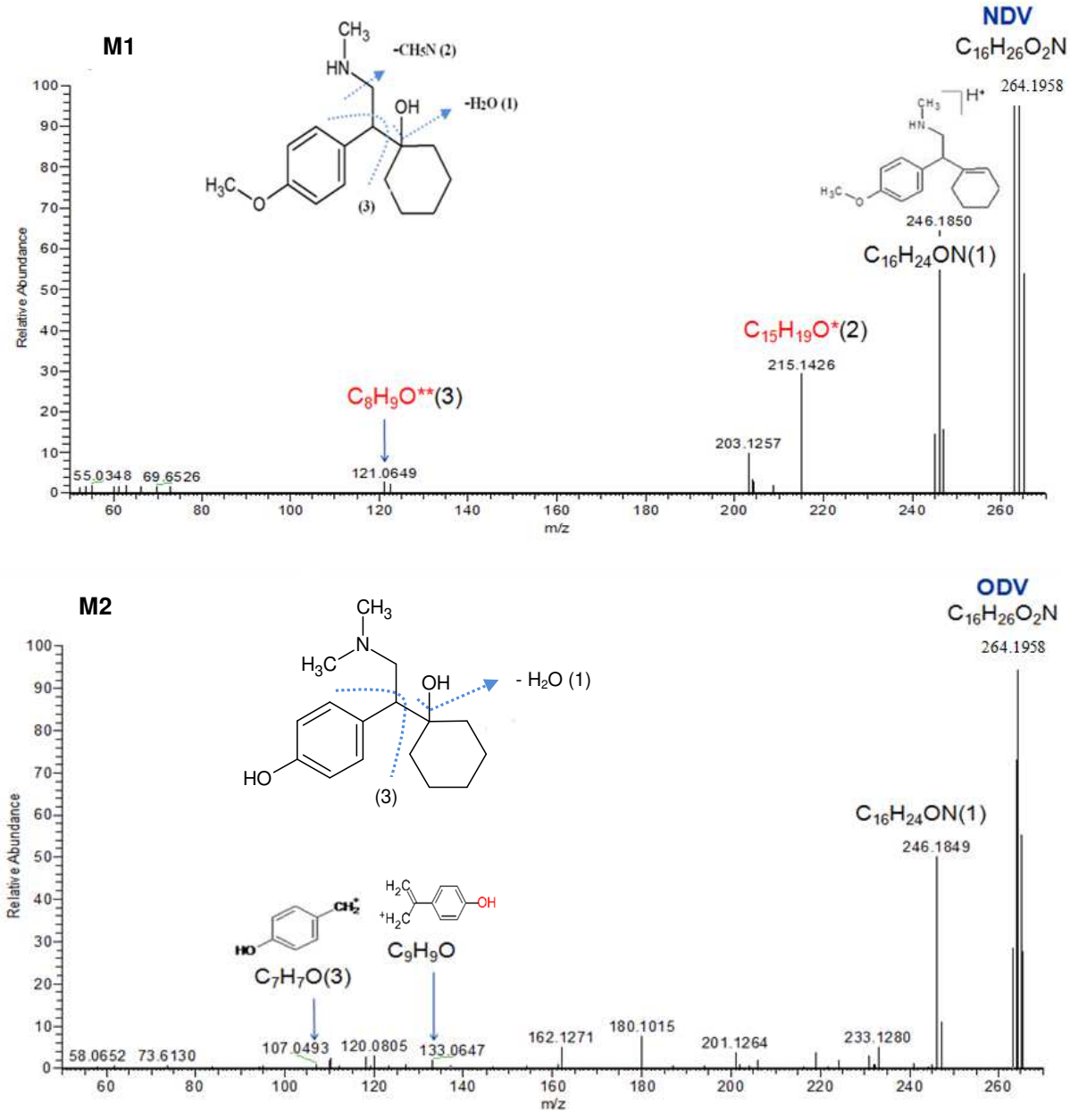

Figure 3. Relevant ions from the high resolution mass spectrum of fragmented NDV (**M1**) and ODV (**M2**) at 10 eV. Asterisks indicate fragments in common with the VEN fragmented spectrum.

340

Table 3 Overview of VEN and its biotransformation products identified in mussel tissues by non-targeted analysis.

341

Peak ID	Tr (min)	Assignment	Elemental composition	Chemical Structure	Measured [M+H]+ (Δm)	Fold change	Relevant $[M+H]^+$ fragment m/z, HCD 10 eV (Δm)	log D_{ow} at pH 2[c]	Tr predicted	ΔTr |observed-predicted|<2	Confidence level
M	14.23	VEN	$C_{17}H_{27}NO_2$	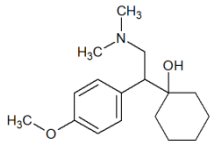	278.2114 (0.0 mmu)	132	260.2007 (0.7 mmu) 215.1427 (0.9 mmu) 121.0646 (0.7 mmu)	-0.62	13.15	1.08	Level 1
M1	12.08	NDV	$C_{16}H_{25}NO_2$	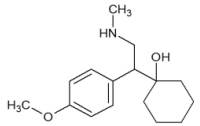	264.1958 (0.0 mmu)	24	246.1850 (0.8 mmu) 215.1426 (1.0 mmu) 121.0649 (0.4 mmu)	-0.55	13.02	0.94	Level 1
M2	8.02	ODV	$C_{16}H_{25}NO_2$	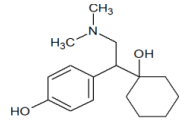	264.1958 (0.0 mmu)	43	246.1849 (0.9 mmu) 133.0647 (0.6 mmu) 107.0493 (0.4 mmu)	-1.36	9.20	1.18	Level 1
M3	14.11	OH-VEN	$C_{17}H_{27}NO_3$	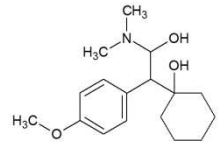	294.2064 (0.0 mmu)	1214	276.1952 (1.1 mmu) 233.1530 (1.1 mmu) 215.1425 (1.1 mmu) 178.1222 (1.0 mmu) 121.0644 (0.9 mmu)	-0.86	12.53	1.58	Level 2
M4	4.85	OH-VEN	$C_{17}H_{27}NO_3$	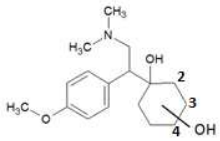	294.2064 (0.0 mmu)	11	276.1955 (0.8 mmu) 121.0644 (0.9 mmu)	-2.05 (2) -2.06 (3) -1.98 (4)	6.93 (2) 6.88 (3) 7.26 (4)	2.1 (2) 2.0 (3) 2.4 (4)	Level 3

342

343

In these conditions, greater chromatographic retention was observed for the N-demethylated metabolite (M1;Tr: 12.08 min) compared to the O-demethylated metabolite (M2;Tr: 8.02 min) (Table 3). For M1, three fragments were highlighted (Fig. 3), with the first one noted at m/z 246.1850, corresponding to H_2O loss. The second one was detected at m/z 215.1426, correponding to the elemental composition $C_{15}H_{19}O$. This fragment resulted from a CH_5N loss consecutive to water loss, as observed with VEN but for a dealkylated metabolite, thus confirming N-dealkylation. The last fragment was detected at m/z 121.0649, corresponding to the elemental composition fragment C_8H_9O already observed for VEN (Fig. 3).

Concerning M2, a fragment was observed at m/z 246.1849 (equivalent to loss of H_2O). HCDfragmentation demonstrated the presence of a second fragment at m/z 133.0647. With the assistance of Xcalibur software, the elemental composition proposed as the first option for this fragment was C_9H_9O (with a delta mm of -0.091) (Fig. 3) . Finally, a fragment was detected at m/z 107.0493 and associated with the elemental composition fragment C_7H_7O, as observed with VEN but for a dealkylated metabolite. The presence of this fragment confirmed that a methyl group was detached from the oxygen of the VEN structure. The injection of analytical standards of NDV and ODV confirmed the identity of these metabolites at a confidence level of 1 in mussel tissues.

3.3.2.1 Oxidative metabolism-hydroxylation

Two metabolites, i.e. M3 and M4, revealed a $[M+H]^+$ of 294.2064. The M3 fold change value was higher than reported for M4, however both were greater than 10 (Table 3) and were detected only in the exposed samples (Fig. 1). The peak shapes and retention times of these signals (M3 and M4) differed from those observed for VEN, indicating that they were potential metabolites (Fig.1, Fig. 4 and Table 3). These metabolites presented a mass shift of +15.9950 compared to VEN. This mass shift could be associated with the biotransformation of an RH structure into an ROH structure, leading to the formation of potential hydroxylated metabolites. M3 and M4 exhibited shorter retention times than VEN, thus supporting the VEN hydroxylation hypothesis. Previous studies have highlighted the formation of such metabolites in organisms such as crustaceans (Jeon et al., 2013) and juvenile lean marine fish (Santos et al., 2020).

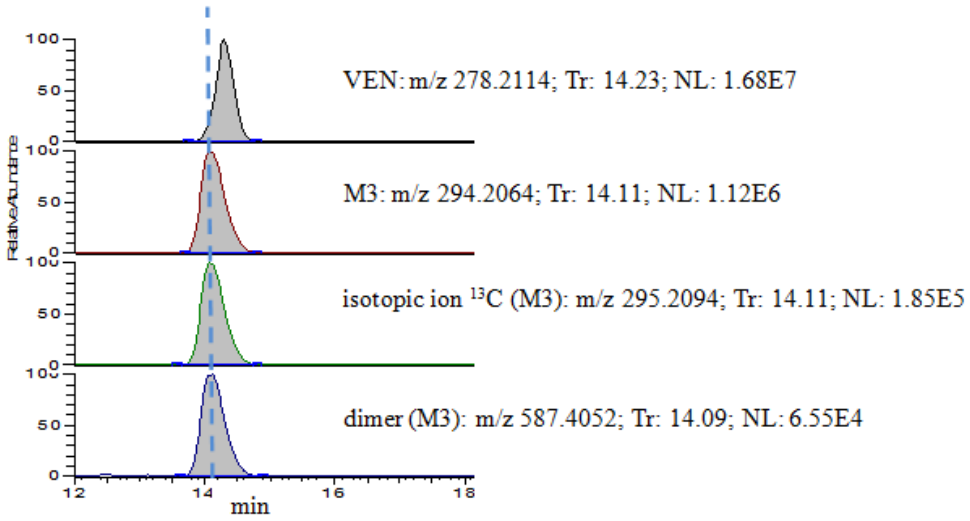

Figure 4. Chromatogram of signals associated with M3 (13C isotopic ion and dimer). Comparison with VEN (Tr= retention time and NL=signal strength).

The addition of an OH group increases the molecular polarity, leading to earlier elution of the molecule in the reverse phase liquid chromatography system used. M3 showed a retention time of 14.11 min, while lower chromatographic retention was obtained for M4 (Tr: 4.85 min). The difference in retention times between M3 and M4 indicated that hydroxylation occurred at different positions in the parent compound (VEN).

For M3, two signals corresponding to (1) the ^{13}C isotopic ion ($[M+H]^+$ 295.2094), and (2) the molecular dimer ($[M+H]^+$ 587.4052) observed at 14.11 min and 14.09 min, respectively, reconfirmed the presence of this potential metabolite (Fig. 4). HCD fragmentation of M3 showed a set of five fragments that allowed us to determine the position of the OH group in its structure (Fig. 5). The fragment at m/z 276.1952 corresponded to H_2O loss from the initial molecule. The fragments observed at m/z 215.1425 and 121.0644 in M1 were common to those of VEN. These coincidences between M3 and VEN fragments were evidence of the absence of OH group on the aromatic ring and on the hexane cycle of the initial molecule. The elementary compositions $C_{15}H_{21}O_2$ and $C_{11}H_{16}ON$ associated with fragments m/z 233.1530 and 178.1222, respectively, confirmed the position of the OH group in the carbon adjacent to the VEN amino group.

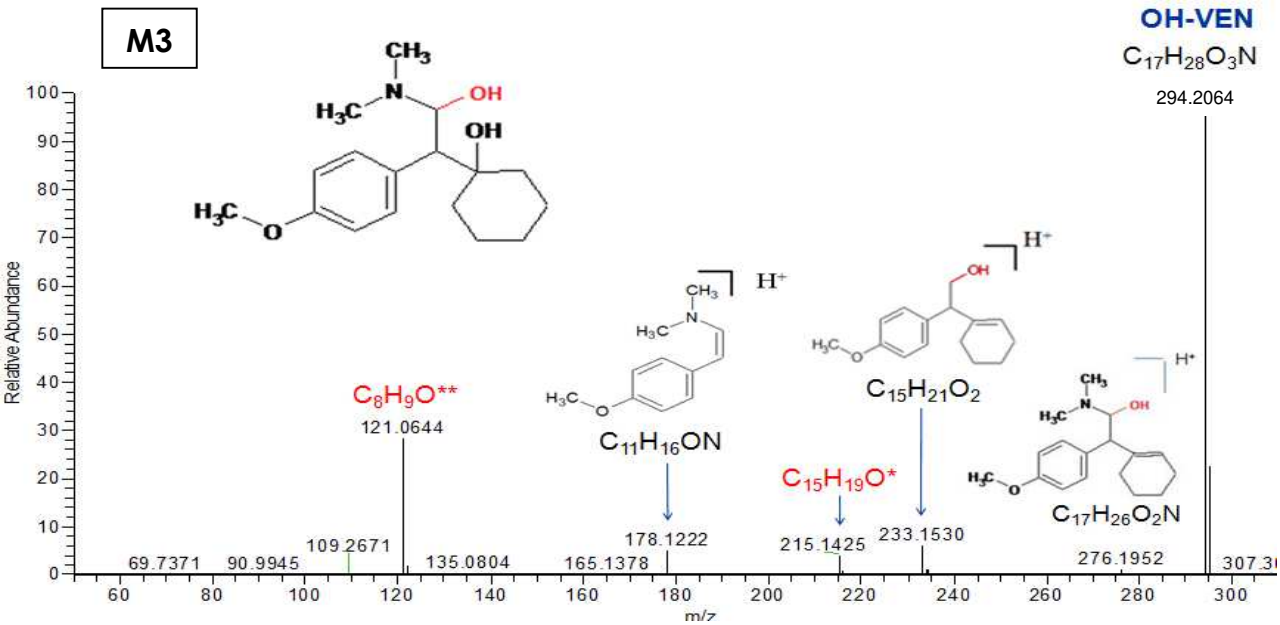

Figure 5. Relevant ions from the high resolution mass spectrum of fragmented M3 at 10 eV. The asterisks indicate fragments in common with the VEN fragmented spectrum.

In addition, in the absence of an analytical standard to ensure the identity of M3 at the maximum confidence level (level 1), a predictive chromatographic retention time model was applied to support our structure proposal for M3. This Tr prediction methodology was from Jeon et al. (2013). The chromatographic retention time was predicted using a multiple regression equation (Eq.1) formulated by plotting the retention time versus the molecular weight and the predicted log D_{ow} of each compound with the available analytical standard (Table 1).

$$\text{Retention time (Tr)} = 4.7107x \log D_{ow} + 0.0324x\ M\ (g/mol) + 7.0762\ (r^2\text{: } 0.92) \quad \text{(Eq.1)}$$

If the Tr predicted for the elucidated structure was within 2 min of the observed Tr, we considered that it was a viable structure. The proposed M3 structure demonstrated a predicted log D_{ow} of -0.86 and a predicted Tr of 12.53 min, showing a difference of less than 2 min with respect to the observed Tr (Table 3). The proposed M3 structure was therefore feasible with a confidence level of 2.

The information available for M4 was limited. The signal intensity was very weak, which made it difficult to identify the relevant fragments. Only two fragments were identified. The experimental mass $[M+H]^+$ 276.1955 was associated with the H_2O loss. A second fragment was observed at m/z

121.0644 and its elemental composition was C_8H_9O, as observed for VEN. The presence of this last fragment suggests that the additional OH group was not positioned in the aromatic ring. Three possible OH group positions were noted for M3 when applying the predictive chromatographic retention time model (Table 3). The M3 structure with the OH group at positions 2 and 3 of the hexane cycle showed predicted retention times at 6.93 min and 6.88 min, respectively (Table 3). Both positions had a delta retention time (calculated considering the observed and predicted value) of 2 min and might have fit a possible M4 structure. Due to the limited information available, the proposed M4 structure had a confidence level of 3.

3.4 Venlafaxine metabolite quantification

The two phase I metabolites generated by demethylation of VEN previously highlighted in mussel tissues were quantified on each exposure day (days 3 and 7). Mean concentrations of NDV (50 ± 13 and 34 ± 13 µg/kg dw) and ODV (28 ± 7 and 24 ± 8 µg/kg) were measured in tissues exposed to VEN for 3 and 7 days (Table 2). Considering the intensity obtained for hydroxylated M3 (i.e. $1.5*10^6$ versus $5*10^5$ for M1), it seems (hypothesis put forward in the absence of absolute quantification) that it was the most abundant of all of the metabolites identified in this study. However, M3 quantification was not possible due to the lack of a commercially available analytical standard.

4. Discussion

PhACs for human care such as VEN are continuously disseminated in the environment (Čelić et al., 2019; Paíga et al., 2016, Santos et al., 2016), resulting in high exposure of non-targeted organisms to these pollutants, even at low concentrations. VEN has been demonstrated to bioaccumulate and interact at the molecular level with aquatic organisms, thereby impacting their tissue metabolic capacities and jeopardizing their adaptive reponse to an acute stressor, as noted by Best et al. (2014) and Ings et al. (2012). In addition, VEN has been shown to have an impact on the behavior (Malvault et al., 2018), reproduction (Parrott and Metcalfe, 2017) and survival (Schultz et al., 2011) of these organisms, but little information is available on the VEN metabolism process involved. In-depth knowledge on the metabolism of this substance in wildlife is necessary to unravel key events in the potential toxicological pathways. Metabolic studies in a broad range of organism are very challenging

but could benefit from advances in chemical analysis and combined targeted and non-targeted approaches, the latter recently used to elucidate small molecules such as metabolites (Bonefille et al., 2017; Santos et al., 2020). The present study in a marine invertebrate illustrates the potential offered by these non-targeted approaches for biomonitoring and conducting surveys on the marine environment.

The sample treatment step is crucial in the determination of unknown metabolites. The tissue treatment method was developed based on the physicochemical properties of known VEN metabolites in the human body (five phase I and two phase II metabolites). These compounds showed medium to high polarity, so the MeOH solvent was ideal for their extraction. VEN and its metabolites have a basic character due to the amine functional group present in their structures. A pH at least two units lower than the pKa value favors the presence of a positive charge on the nitrogen of the amine group of these compounds. Since the compounds of interest hadthis property, the sorbent SPE chosen combined two mechanisms to enhance their retention, i.e. strong cation exchange and hydrophobic interactions. This double retention mechanism enabled the recovery of phase I metabolites, but also of glucuronide metabolites, which are highly complex due to their elevated polarity and sensitivity to hydrolysis during the extraction process (Karinen et al., 2009; Ketola and Hakala, 2010). The analytical method performance evaluation showed that the combined tissue extraction and purification conditions enabled high absolute recoveries of phase I metabolites and glucuronide metabolites, along with moderate matrix effects.

Application of the tissue treatment method to the VEN-exposed samples generated data that helped determine the extent of parent compound accumulation in mussel tissues. The BCF values obtained (177 ± 27 L/kg dw and 229 ± 29 L/kg dw for VEN exposure at days 3 and 7, respectively) were in a range similar to those already reported for VEN-exposed mussels. A first study conducted in mussels (*M. galloprovincialis*) exposed for 7 days to 1, 10 and 100 µg/L VEN reported BCF values of 178 ± 8.0 L/kg dw, 146 ± 35 L/kg dw and 189 ± 15 L/kg dw, respectively (Gomez et al, submitted). In a second study, the BCF values reported for mussels (*M. galloprovincialis*) exposed for 20 days to 10.7 ± 1.6 µg/L of VEN were between 213.3 and 528.1 L/kg dw for the different treatments applied while also taking the effects of water warming and acidification into account (Serra-Compte et al., 2018). The authors suggested that the positive ionized form of VEN would facilitate its adhesion to the biological matrix, which could explain the high BCF value obtained.

493 The high VEN bioconcentration combined with the presence of cytochrome P450 in mussels favours
494 enzymatic reactions involved in the metabolism of this xenobiotic compound in mussels (Snyder,
495 2000). The application of a non-targeted approach to samples collected in VEN-exposed mussels led
496 to the identification of four phase I metabolites. Two metabolites resulted from the demethylation
497 process at two different VEN positions: N-demethylation and O-demethylation. These metabolites
498 have already been previously identified in laboratory-exposed mussels (Serra-Compte et al., 2018;
499 Gomez et al., submitted) and in mussels collected in coastal areas of France (Martínez Bueno et al.,
500 2014), Portugal, Italy and Spain (Álvarez-Muñoz et al., 2015b). Both metabolites presented
501 concentrations two orders of magnitude lower than the parent molecule. This behavior may be
502 expected in the mussel detoxification process, where it is sought to produce more hydrophilic and less
503 toxic metabolites, thereby facilitating their excretion. Quantification of these metabolites showed that,
504 for both exposure days, in the tested mussels there was a slight trend in favor of the detoxification
505 pathway that generates VEN dealkylation at the nitrogen position, whereas ODV is the major
506 metabolite in humans (Sangkuhl et al., 2014). A similar behavior was observed by Santos et al.
507 (2020), showing that N-demethylated metabolites are the predominant ones in fish. They suggest that
508 due to the higher hydrophilic character of NDV at physiological pH compared to ODV, fish prefer to
509 metabolize venlafaxine to NDV, generating higher concentrations of this metabolite in fish. The above
510 explanation could potentially be the justification for the higher presence of NDV evidenced in mussels.
511 Finally, NDV and ODV metabolites were both formed early during the detoxification process since they
512 both presented higher concentrations at day 3. This was already observed in a previous study (Gomez
513 et al., submitted). However, the findings of the non-parametric statistical Mann Whitney test comparing
514 data obtained on days 3 and 7 revealed no significant differences between these days.

515 The two other metabolites identified were hydroxylated VEN metabolites at two different positions: 1)
516 on the carbon adjacent to the amine group, and 2) on the hexane cycle. Hydroxylation is one of the
517 two known N-dealkylation mechanisms. This mechanism involves formal hydroxylation of a C-H bond
518 on the carbon adjacent to the heteroatom (HAT, H-atom transfer) (Meunier et al., 2004). The above
519 findings support the hypothesis of the proposed structure for the VEN hydroxylated metabolite (M3),
520 which to our knowledge has not been previously described. This metabolite showed the highest
521 intensities of all metabolites identified in the study for both exposure days. Hydroxylated metabolites
522 were also shown to be major diclofenac metabolites in mussels (Bonnefille et al., 2017; Świacka et al.,

2019). This also highlights the differences in biotransformation processes in mussels compared to humans (Sangkuhl et al., 2014). Due to the low intensity of the second hydroxylated venlafaxine metabolite (M4), there was not a sufficient number of fragments to increase the confidence level for the suggested structure. This hydroxylated metabolite has been previously identified in crustaceans (Jeon et al., 2013). Both hydroxylated metabolites (M3 and M4) were formed later during the detoxification process since they both showed higher intensities at day 7.

No glucuronide metabolites were detected despite the fact that the method was found to be able to retain glucuronide metabolites. This could possibly be explained by two hypotheses: 1) mussels are not capable of producing glucuronides, or 2) the concentration at which these compounds are formed is below the detection limit of our method. A previous study revealed that mussels are capable of generating glucuronide metabolites from xenobiotic benzo(a)pyrene (Michel et al., 1995). Mussels may therefore possibly be able to generate this type of metabolite from pharmaceuticals. The above suggests that the concentration of these metabolites in the analyzed tissues was lower than our detection limit.

5. Conclusions

The non-targeted approach was demonstrated to be a relevant method for characterizing and identifying VEN metabolites produced in Mediterranean mussels, thereby generating insight into the VEN metabolism in mussels. Two hydroxylated metabolites were identified for the first time in this organism, thus confirming its ability to efficiently dealkylate and then hydroxylate amino pharmaceuticals. However, glucuronidation did not appear to be a major detoxification pathway for these compounds. Our results showed that mussels did not share the same VEN metabolism pathway as in humans, and N-demethylation appeared to be the main metabolization pathway in Mediterranean mussels. This hydroxylation ability thus facilitates further interpretation of metabolism in mussels. The identified metabolites could also be used as biomarkers of exposure to environmental pollutants. It should be noted that despite the active metabolism of mussels, venlafaxine bioaccumulates 117 times in this organism. This warrants further studies on the effects of these metabolites and venlafaxine in mussels.

Acknowledgments

The authors would like to thank the French National Research Agency (IMAP ANR-16-CE34-0006-01) and *Vicerrectoría de Investigación y Extensión del Instituto Tecnológico de Costa Rica* for funding. We also thank David Rosain and Céline Roques of the University of Montpellier for technical assistance in the laboratory and David Manley, English translator, for reviewing this document. The analyses were performed at the Platform Of Non-Target Environmental Metabolomics (PONTEM) member of the BioCampus Montpellier Alliance for Metabolomics and Metabolims Analysis (MAMMA) facility, Montpellier (France). This work benefitted from the French "Aquatic Ecotoxicology" framework which aims at fostering stimulating scientific discussions and collaborations in favor of more integrative approaches.

References

Alvarez-Muñoz, D., Huerta, B., Fernandez-Tejedor, M., Rodríguez-Mozaz, S., Barceló, D., 2015a. Multi-residue method for the analysis of pharmaceuticals and some of their metabolites in bivalves. Talanta 136, 174–182.

Álvarez-Muñoz, D., Rodríguez-Mozaz, S., Maulvault, A.L., Tediosi, A., Fernández-Tejedor, M., Van den Heuvel, F., Kotterman, M., Marques, A., Barceló, D., 2015b. Occurrence of pharmaceuticals and endocrine disrupting compounds in macroalgaes, bivalves, and fish from coastal areas in Europe. Environ. Res. 143, 56–64.

Best, C., Melnyk-Lamont, N., Gesto, M., Vijayan, M.M., 2014. Environmental levels of the antidepressant venlafaxine impact the metabolic capacity of rainbow trout. Aquat. Toxicol. 155, 190–198.

Bonnefille, B., Arpin-Pont, L., Gomez, E., Fenet, H., Courant, F., 2017. Metabolic profiling identification of metabolites formed in Mediterranean mussels (*Mytilus galloprovincialis*) after diclofenac exposure. Sci. Total Environ. 583, 257–268.

Brieudes, V., Lardy-Fontan, S., Vaslin-Reimann, S., Budzinski, H., Lalere, B., 2017. Development of a multi-residue method for scrutinizing psychotropic compounds in natural waters. J. Chromatogr. B Anal. Technol. Biomed. Life Sci. 1047, 160–172.

Čelić, M., Gros, M., Farré, M., Barceló, D., Petrović, M., 2019. Pharmaceuticals as chemical markers of wastewater contamination in the vulnerable area of the Ebro Delta (Spain). Sci. Total Environ. 652, 952–963.

580 Courant, F., Antignac, J.-P., Dervilly-Pinel, G., Le Bizec, B., 2014. Basics of mass spectrometry based
581 metabolomics. Proteomics 14:2369–2388.

582 Gomez, E., Bachelot, M., Boillot, C., Dominique, M., Chiron, S., Casellas, C., Fenet, H., 2012.
583 Bioconcentration of pharmaceuticals (benzodiazepines) and two personal care products (UV
584 filters) in marine mussels (*Mytilus galloprovincialis*) under controlled laboratory
585 conditions).Environ. Sci. Pollut. Res. 19:2561-2569.

586 Gomez, E., Boillot, C., Martinez Bueno, MJ., Munaron, D., Mathieu, O., Courant, F., Fenet, H. In vivo
587 exposure of marine mussel to venlafaxine: bioconcentration and metabolization. Sumitted

588 Ings, J.S., George, N., Peter, M.C.S., Servos, M.R., Vijayan, M.M.Venlafaxine and atenolol disrupt
589 epinephrine-stimulated glucose production in rainbow trout hepatocytes. Aquat. Toxicol. 106-
590 107, 48-55.

591 Jeon, J., Kurth, D., Hollender, J., 2013. Biotransformation pathways of biocides and pharmaceuticals
592 in freshwater crustaceans based on structure elucidation of metabolites using high resolution
593 mass spectrometry. Chem. Res. Toxicol. 26, 313–324.

594 Karinen, R., Andersen, J.M., Ripel, Å., Hasvold, I., Hopen, A.B., Mørland, J., Christophersen, A.S.,
595 2009. Determination of heroin and its main metabolites in small sample volumes of whole blood
596 and brain tissue by reversed-phase liquid chromatography-tandem mass spectrometry. J. Anal.
597 Toxicol. 33, 345–350.

598 Ketola, R., Hakala, K., 2010. Direct analysis of glucuronides with liquid chromatography-mass
599 spectrometric techniques and methods. Curr. Drug Metab. 11, 561–582.

600 Martínez Bueno, M.J., Boillot, C., Munaron, D., Fenet, H., Casellas, C., Gómez, E., 2014. Occurrence
601 of venlafaxine residues and its metabolites in marine mussels at trace levels: Development of
602 analytical method and a monitoring program. Anal. Bioanal. Chem. 406, 601–610.

603 Maulvault, A.L., Santos, L.H.M.L.M., Paula, J.R., Camacho, C., Pissarra, V., Fogaça, F., et al., 2018.
604 Differential behavioural responses to venlafaxine exposure route, warming and acidification in
605 juvenile fish (Argyrosomus regius). Sci. Total Environ. 634, 1136–1147

606 McEneff, G., Barron, L., Kelleher, B., Paull, B., Quinn, B., 2013. The determination of pharmaceutical
607 residues in cooked and uncooked marine bivalves using pressurised liquid extraction, solid-

608 phase extraction and liquid chromatography-tandem mass spectrometry. Anal. Bioanal. Chem.
609 405, 9509–9521.

610 Meunier, B., de Visser, S.P., Shaik, S., 2004. Mechanism of oxidation reactions catalyzed by
611 cytochrome P450 enzymes. Chem. Rev. 104, 3947–3980.

612 Michel, X.R., Beasse, C., Narbonne, J., 1995. In vivo metabolism of benzo (a) pyrene in the mussel
613 *Mytilus galloprovincialis*. Arch. Environ. Contam. Toxicol. 28, 215–222.

614 Moreno-González, R., Rodríguez-Mozaz, S., Huerta, B., Barceló, D., León, V.M., 2016. Do
615 pharmaceuticals bioaccumulate in marine molluscs and fish from a coastal lagoon? Environ.
616 Res. 146, 282–298.

617 Paíga, P., Santos, L.H.M.L.M., Ramos, S., Jorge, S., Silva, J.G., Delerue-Matos, C., 2016. Presence
618 of pharmaceuticals in the Lis river (Portugal): sources, fate and seasonal variation. Sci. Total
619 Environ. 573, 164–177.

620 Paíga, P., Correia, M., Fernandes, M., Silva, A., Carvalho, M., Vieira, J., Jorge, S., Silva, J., Freire, C.,
621 Delerue-Matos, C., 2019. Assessment of 83 pharmaceuticals in WWTP influent and effluent
622 samples by UHPLC-MS/MS : Hourly variation. Sci. Total Environ. 648, 582–600.

623 Parrott, J.L., Metcalfe, C.D., 2017. Assessing the effects of the antidepressant venlafaxine to fathead
624 minnows exposed to environmentally relevant concentrations over a full life cycle. Environ.
625 Pollut. 229, 403–411.

626 Sangkuhl, K., Stingl, J., Turpeinen, M., Altman, R., Klein, T., 2014. PharmaGKB summary: venlafaxine
627 pathway. Pharmacogenet Genom. 24, 62–72.

628 Santos, L.H.M.L.M., Ramalhosa, M.J., Ferreira, M., Delerue-Matos, C., 2016. Development of a
629 modified acetonitrile-based extraction procedure followed by ultra-high performance liquid
630 chromatography–tandem mass spectrometry for the analysis of psychiatric drugs in sediments.
631 J. Chromatogr. A 1437, 37–48.

632 Santos, L.H.M.L.M., Maulvault, A.L., Jaén-Gil, A., Marques, A., Barceló, D., Rodríguez-Mozaz, S.,
633 2020. Insights on the metabolization of the antidepressant venlafazine by meagre (Argyrosomus
634 regius) using a combined target and suspect screening approach. Sci. Total Environ. 737,
635 140226

Schultz, M.M., Painter, M.M., Bartell, S.E., Logue, A., Furlong, E.T., Werner, S.L., et al., 2011. Selective uptake and biological consequences of environmentally relevant antidepressant pharmaceutical exposures on male fathead minnows. Aquat. Toxicol. 104, 38–47.

Schymanski, E.L., Jeon, J., Gulde, R., Fenner, K., Ru, M., Singer, H.P., Hollender, J., 2014. Identifying Small Molecules via High Resolution Mass Spectrometry: Communicating Confidence. Environ. Sci. Technol. 48, 2097–2098.

Serra-Compte, A., Maulvault, A.L., Camacho, C., Álvarez-Muñoz, D., Barceló, D., Rodríguez-Mozaz, S., Marques, A., 2018. Effects of water warming and acidification on bioconcentration, metabolization and depuration of pharmaceuticals and endocrine disrupting compounds in marine mussels (*Mytilus galloprovincialis*). Environ. Pollut. 236, 824–834.

Silva, L.J.G., Martins, M.C., Pereira, A.M.P.T., Meisel, L.M., Gonzalez-Rey, M., Bebianno, M.J., Lino, C.M., Pena, A., 2016. Uptake, accumulation and metabolization of the antidepressant fluoxetine by *Mytilus galloprovincialis*. Environ. Pollut. 213, 432–437.

Snyder, M.J., 2000. Cytochrome P450 enzymes in aquatic invertebrates: Recent advances and future directions. Aquat. Toxicol. 48, 529–547.

Świacka, K., Szaniawska, A., Caban, M., 2019. Evaluation of bioconcentration and metabolism of diclofenac in mussels *Mytilus trossulus* - laboratory study. Mar. Pollut. Bull.141, 249–255.

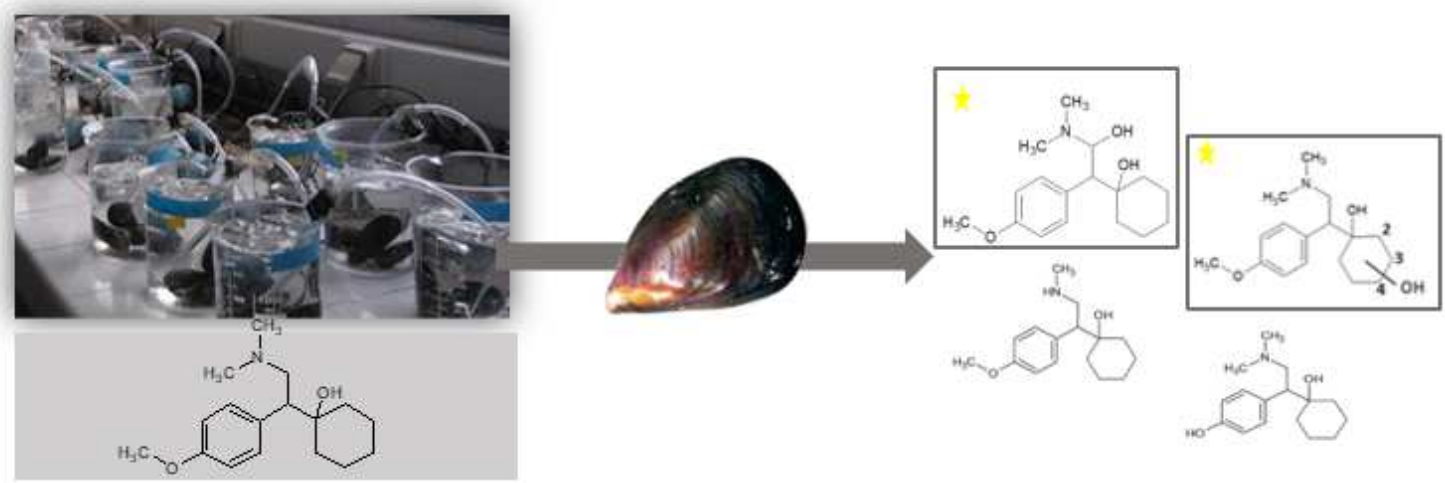
CH3
H3C
N
OH
H3C
O
OH
HN
HO
2
3
4